Preparation and Some Properties of Linear-Type S-Bridged $Ir^{III}Co^{III}Ir^{III}$ Trinuclear Complexes with 2-Aminoethanethiolate (aet) or L-Cysteinate (L-cys). Crystal Structure of $\Delta\Lambda$-$[Co\{Ir(aet)_3\}_2](NO_3)_3$

Takumi KONNO,* Kenji NAKAMURA, Ken-ichi OKAMOTO, and Jinsai HIDAKA
Department of Chemistry, University of Tsukuba, Tsukuba, Ibaraki 305
(Received May 13, 1993)

The reactions of newly prepared *fac*(*S*)-$[Ir^{III}(aet)_3]$ or Δ_{LLL}-*fac*(*S*)-$[Ir^{III}$(L-cys-*N*,*S*)$_3]^{3-}$ with Co^{2+}, followed by the air or H_2O_2 oxidation, gave linear-type S-bridged trinuclear complexes, $[Co^{III}\{Ir^{III}(aet)_3\}_2]^{3+}$ and $\Delta_{LLL}\Delta_{LLL}$-$[Co^{III}\{Ir^{III}$(L-cys-*N*,*S*)$_3\}_2]^{3-}$. The aet trinuclear complex was separated and optically resolved into the $\Delta\Lambda$, $\Delta\Delta$, and $\Lambda\Lambda$ isomers and the crystal structure of the $\Delta\Lambda$ isomer was determined by X-ray diffraction. $[Co\{Ir(aet)_3\}_2](NO_3)_3\cdot 2H_2O$, chemical formula $C_{12}H_{40}N_9S_6O_{11}CoIr_2$, crystallizes in the triclinic, space group $P\bar{1}$ with $a=8.945(2)$, $b=12.073(3)$, $c=8.849(3)$ Å, $\alpha=110.36(2)$, $\beta=102.55(2)$, $\gamma=70.88(2)°$, $U=841(2)$ Å^3, $Z=1$, and $R=0.059$. The central Co(III) has a trigonally distorted octahedral geometry, coordinated by six thiolato sulfur atoms from the octahedral Δ- and Λ-*fac*(*S*)-$[Ir(aet)_3]$ terminals. The other trinuclear complexes were characterized by their absorption, CD, and ^{13}C NMR spectra. The meso–racemic isomerization, which results from the cleavage of the Co–S bonds, was recognized for $[Co\{Ir(aet)_3\}_2]^{3+}$ in D_2O, methanol–H_2O, and ethanol–H_2O. The cyclic voltammogram of *rac*-$[Co\{Ir(aet)_3\}_2]^{3+}$ in water showed two almost reversible redox couples at −0.23 V and +0.73 V (vs. Ag/AgCl). The chemical properties of the present $Ir^{III}Co^{III}Ir^{III}$ complexes are discussed in comparison with those of the corresponding $Rh^{III}Co^{III}Rh^{III}$ and $Co^{III}Co^{III}Co^{III}$ complexes.

It has been shown that the coordinated thiolato sulfur atoms in *fac*(*S*)-$[Co(aet)_3]$ (aet = 2-aminoethanethiolate; $NH_2CH_2CH_2S^-$),[1—11] *fac*(*S*)-$[Co$(L-cys-*N*,*S*)$_3]^{3-}$ (L-cys = L-cysteinate; $NH_2CH(COO^-)$-CH_2S^-),[8,9,12—14] *fac*(*S*)-$[Rh(aet)_3]$,[15—19] and *fac*(*S*)-$[Rh$(L-cys-*N*,*S*)$_3]^{3-}$[15] possess an ability to bind to another metal ions, forming a variety of S-bridged polynuclear complexes. For example, the reactions of these mononuclear complexes with a metal ion M′=Fe(III), Co(II), Co(III), or Ni(II) produce well-known linear-type S-bridged trinuclear complexes, $[M'\{M$(aet or L-cys-*N*,*S*)$_3\}_2]^{n+\text{ or }n-}$, in which the terminal *fac*(*S*)-$[M$(aet or L-cys-*N*,*S*)$_3]^{0\text{ or }3-}$ function as a S-donating terdentate ligand to a central metal ion M′.[1—8,11—15] In a previous paper,[15] we have pointed out that the $Rh^{III}Co^{III}Rh^{III}$ trinuclear complexes, $[Co\{Rh$(aet or L-cys-*N*,*S*)$_3\}_2]^{3+\text{ or }3-}$, exhibit different spectrochemical and electrochemical behavior from the corresponding $Co^{III}Co^{III}Co^{III}$ complexes, $[Co\{Co$(aet or L-cys-*N*,*S*)$_3\}_2]^{3+\text{ or }3-}$. In order to elucidate the correlations among the structural, spectrochemical, and electrochemical properties of these S-bridged trinuclear complexes, it is desirable to introduce *fac*(*S*)-$[Ir$(aet or L-cys-*N*,*S*)$_3]^{0\text{ or }3-}$ in the trinuclear structure, which brings completion to a series of the linear-type S-bridged $M^{III}Co^{III}M^{III}$ complexes (M = Co, Rh, or Ir). In this paper, we report on the synthesis of the novel linear-type $Ir^{III}Co^{III}Ir^{III}$ complexes,$[Co\{Ir$(aet or L-cys-*N*,*S*)$_3\}_2]^{3+\text{ or }3-}$, from newly prepared *fac*(*S*)-$[Ir$(aet or L-cys-*N*,*S*)$_3]^{0\text{ or }3-}$ and Co(II), along with their chemical characterization and single-crystal structural analysis.

Experimental

Preparation of Complexes. ***fac*(*S*)-$[Ir(aet)_3]$ (1).** To a solution containing 2.5 g (32.7 mmol) or 2-aminoethanethiol (Haet) and 2.2 g of NaOH in 60 cm^3 of water was added 2.0 g (6.7 mmol) of $IrCl_3$. The mixture was continuously stirred at 110 °C in an oil bath for 2 d under a nitrogen atmosphere. The resulting ivory white precipitate was collected by filtration and washed with a large amount of water and methanol. Yield: 1.37 g (49 %). Found: C, 17.05; H, 4.43; N, 9.79%. Calcd for $[Ir(C_2H_6NS)_3]$: C, 17.13; H, 4.31; N, 9.99%.

Δ_{LLL}-*fac*(*S*)-$[Ir$(L-cys-*N*,*S*)$_3]^{3-}$ (2). To a solution containing 3.3 g (27.2 mmol) of L-cysteine (L-H_2cys) and 2.2 g of NaOH in 30 cm^3 of water was added 2.0 g (6.7 mmol) of $IrCl_3$. The mixture was continuously stirred at 95 °C in an oil bath for 2 d under a nitrogen atmosphere, which gave a deep yellow-brown solution. After cooling to room temperature, the pH of the reaction solution was adjusted to ca. 2 with 1 mol dm^{-3} HCl. The resulting ivory white precipitate was collected by filtration and washed with a large amount of 1 mol dm^{-3} HCl and methanol. It was found form the QAE-Sephadex A-25 column chromatography and the CD and ^{13}C NMR spectral measurements that this complex contained only the Δ_{LLL}-*fac*(*S*) isomer. Yield: 0.81 g (21%). Found: C, 18.68; H, 3.56; N, 7.10%. Calcd for $H_3[Ir(C_3H_5NO_2S)_3]\cdot H_2O$: C, 18.94; H, 3.53; N, 7.36%.

$[Co\{Ir(aet)_3\}_2]^{3+}$ (3). To a suspension containing 0.3 g (0.71 mmol) of *fac*(*S*)-$[Ir(aet)_3]$ (**1**) in 5 cm^3 of water was added a solution containing 0.15 g (0.41 mmol) of $Co(NO_3)_2\cdot 6H_2O$ in 1 cm^3 of water. The mixture was stirred at room temperature for 10 min, during which time the ivory white suspension became a deep purple solution and dark purple precipitate appeared.[20] The addition of 1.5 cm^3 of 3% H_2O_2 to the dark purple suspension, followed by stirring at room temperature for 1 h, gave deep dark green solution.[21] The dark green solution was then poured onto a SP-Sephadex C-25 column (Na^+ form, 5 cm×90 cm). After sweeping the column with water, the adsorbed band was eluted with a 0.3 mol dm^{-3} aqueous solution of NaCl or

$NaNO_3$. Only two bands, **3a** (dark brown) and **3b** (dark green), were eluted in this order, while a faint brown band was adsorbed on the top of the column. The formation ratio of **3a** and **3b** was about 1:2. Each eluate was concentrated to a small volume with a rotary evaporator and the deposited NaCl or $NaNO_3$ was filtered off. The filtrate was stored in a refrigerator for several days and the resulting black crystals were collected by filtration. One of the crystals of **3a**$(NO_3)_3$ was used for X-ray analysis. Found for **3a**$(NO_3)_3$: C, 12.39; H, 3.77; N, 10.75%. Calcd for $[Co\{Ir(C_2H_6NS)_3\}_2](NO_3)_3\cdot 4H_2O$: C, 12.44; H, 3.83; N, 10.89%. Found for **3b**$(NO_3)_3$: C, 12.47; H, 3.33; N, 11.35%. Calcd for $[Co\{Ir(C_2H_6NS)_3\}_2](NO_3)_3\cdot H_2O\cdot 0.5NaNO_3$: C, 12.57; H, 3.34; N, 11.60%. Found for **3a**Cl_3: C, 13.64; H, 3.79; N, 8.19%. Calcd for $[Co\{Ir(C_2H_6NS)_3\}_2]Cl_3\cdot 2H_2O\cdot 0.25NaCl$: C, 13.63; H, 3.81; N, 7.95%. Found for **3b**Cl_3: C, 13.82; H, 3.76; N, 7.95%. Calcd for $[Co\{Ir(C_2H_6NS)_3\}_2]Cl_3\cdot 2H_2O$: C, 13.82; H, 3.87; N, 8.06%.

An aqueous solution of **3b**Cl_3 was charged on a SP-Sephadex C-25 column (Na^+ form, 5 cm×40 cm). Two dark green bands, $(-)^{CD}_{600}$-**3b** and $(+)^{CD}_{600}$-**3b**, were separated by eluting with a 0.075 mol dm^{-3} aqueous solution of $Na_2[Sb_2(R,R\text{-tartrate})_2]\cdot 5H_2O$. After separation into two bands, each adsorbed band was eluted with a 0.3 mol dm^{-3} aqueous solution of NaCl. Each eluate was concentrated to a small volume with a rotary evaporator and the deposited NaCl was filtered off. The filtrate was stored in a refrigerator for several days and the resulting black crystals were collected by filtration. Found for $(-)^{CD}_{600}$-**3b**Cl_3; C, 13.74; H, 3.74; N, 8.13%. Calcd for $[Co\{Ir(C_2H_6NS)_3\}_2]Cl_3\cdot 2H_2O$: C, 13.82; H, 3.87%; N, 8.06%. **3a** was not optically resolved by the SP-Sephadex C-25 column chromatography using a 0.075 mol dm^{-3} aqueous solution of $Na_2[Sb_2(R,R\text{-tartrate})_2]\cdot 5H_2O$ as an eluent.

$\Delta_{LLL}\Delta_{LLL}$-$[Co\{Ir(L\text{-cys-}N,S)_3\}_2]^{3-}$ (4). A 0.1 g (0.43 mmol) sample of Δ_{LLL}-*fac*(*S*)-$H_3[Ir(L\text{-cys-}N,S)_3]\cdot H_2O$ (H_3**2**$\cdot H_2O$) was dissolved in 8 cm^3 of water by adding 4 cm^3 of 1 mol dm^{-3} NaOH. To this was added a solution containing 0.08 g (0.33 mmol) of $CoCl_2\cdot 6H_2O$ in 4 cm^3 of water. The solution color turned immediately from yellow to purple.[22] The mixture was stirred at room temperature for 3 h, during which time the solution color gradually changed to dark green by the air oxidation. After removing insoluble materials by filtration, a large amount of ethanol was added to the filtrate. The resulting dark green precipitate was collected by filtration and recrystallized from water by adding ethanol. It was found form the QAE-Sephadex A-25 column chromatography and the CD spectral measurements of the dark green reaction solution that the $(-)^{CD}_{600}$-$\Delta_{LLL}\Delta_{LLL}$ isomer was selectively formed for $[Co\{Ir(L\text{-cys-}N,S)_3\}_2]^{3-}$. This isomer was also selectively formed when the aqueous mixture of Δ_{LLL}-*fac*(*S*)-$H_3[Ir(L\text{-cys-}N,S)_3]\cdot H_2O$, NaOH, and $CoCl_2\cdot 6H_2O$ was heated at 95 °C for one day under an nitrogen atmosphere, followed by oxidizing with air. Yield: 0.10 g (40%). Found: C, 14.92; H, 3.68; N, 5.69%. Calcd for $Na_3[Co\{Ir(C_3H_5NO_2S)_3\}_2]\cdot 11.5H_2O$: C, 15.07; H, 3.72; N, 5.86%.

Δ_{LLL}-*fac*(*S*)-H_3[Rh(L-cys-*N*,*S*)$_3$],[15] ***rac*-[Co{Co(aet)$_3$}$_2$](NO$_3$)$_3$,**[7] ***rac*- and *ΔΔ*-[Co{Rh(aet)$_3$}$_2$](NO$_3$)$_3$,**[15] were prepared by the methods described in previous papers.

Measurements. The electronic absorption spectra were recorded with a JASCO UVIDEC-610C or JASCO Ubest-55 spectrophotometer, and the CD spectra with a JASCO J-600 spectropolarimeter. The ^{13}C NMR spectra were recorded with a BRUKER-AM-500 NMR spectrometer at a probe temperature in D_2O. Sodium 4,4-dimethyl-4-silapentane-1-sulfonate (DSS) was used as the internal reference. The cyclic voltammograms were recorded with a CV-1B apparatus (Bioanalytical Systems, Inc.) using a grassy-carbon electrode or a platinum microelectrode (Bioanalytical Systems, Inc. GCE or MPTE) as a working electrode. An aqueous Ag/AgCl/NaCl (3 mol dm^{-3}) electrode (Bioanalytical Systems, Inc., RE-1B) and platinum wire were used as reference and auxiliary electrodes, respectively. Electrochemical experiments were conducted at 22 °C in water with 0.1 mol dm^{-3} $NaNO_3$ as the supporting electrolyte and complex concentrations of 1.0 mmol dm^{-3}.

Crystallography. X-Ray Data Collection. A black crystal (ca. 0.50×0.33×0.20 mm) of **3a**$(NO_3)_3$ was used for data collection on an Enraf–Nonius CAD4 diffractometer with a graphite-monochromatized Mo $K\alpha$ radiation (λ=0.71073 Å). Unit cell dimensions were determined by least-squares refinement of 25 reflections with $23°<2\theta<28°$.

Crystal data: $[Co\{Ir(aet)_3\}_2](NO_3)_3\cdot 2H_2O=C_{12}H_{40}N_9S_6O_{11}CoIr_2$, M=1122.3, triclinic, space group $P\bar{1}$ (No. 2), a=8.945(2), b=12.073(3), c=8.849(3) Å, α=110.36(2), β=102.55(2), γ=70.88(2)°, U=841(2) Å^3, Z=1, D_x=2.22 g cm^{-3}, $F(000)$=540, μ(Mo $K\alpha$)=84.64 cm^{-1}, and room temperature.

The intensity data were collected by the ω–2θ scan mode up to 2θ=56° ($-11\leqq h\leqq 11$, $-16\leqq k\leqq 16$, $0\leqq l\leqq 11$) with scan width $(1.10+0.35\tan\theta)°$ and scan rate varied from 1 to 5° min^{-1} (on ω). The intensities were corrected for Lorentz and polarization. An empirical absorption corrections based on a series of ψ scans were applied (max. and min. transmission factors, 1.00 and 0.52). A total of 3817 independent reflections with $|F_o|>3\sigma(|F_o|)$ of the measured 4318 reflections were considered as 'observed' and used for the structure determination.

Determination of Crystal Structure. The iridium, cobalt, and sulfur atoms were located by the direct method of the crystallographic package SDP.[23] The remaining non-hydrogen atoms were found by conventional difference Fourier techniques to give a trial structure. The structure was refined by full-matrix least-squares techniques using SHELX76[24] on a FACOM M1800/20 computer. The oxygen atoms of the nitrate anions were refined isotropically and all other non-hydrogen atoms were refined anisotropically. The cobalt atom was constrained to the special position with a site occupancy factor of 0.5. The nitrogen (N2N) and oxygen (021, 022, 023) atoms of one nitrate anion were refined with a site occupancy factor of 0.5. The ethylene hydrogen atoms in the aet ligands were fixed by geometrical constrains (C–H=0.95 Å) and isotropic thermal parameters (B=3.95 Å^2). The hydrogen atoms attached to the amine nitrogen and water oxygen atoms were not included in the calculation. Neutral atomic scattering factors for cobalt and iridium atoms were taken from the literature,[25] while all others were supplied in SHELX76. The final refinement gave R=0.059 and R_w=0.063 ($w=0.5695/(\sigma^2(F_o)+0.010174|F_o|^2)$; S=0.63.[26] The final difference Fourier maps showed several peaks larger than 1.0 e/Å^3, all in the vicinity of the iridium and cobalt atoms. The final atomic coordinates for non-

Table 1. Final Atomic Coordinates and Equivalent Isotropic ($B_{eq}/Å^2$) or Isotropic ($B/Å^2$) Thermal Parameters for Non-Hydrogen Atoms

$$B_{eq} = (8\pi^2/3)\sum_i\sum_j U_{ij}a_i^*a_j^*\boldsymbol{a}_i\cdot\boldsymbol{a}_j$$

Atom	x	y	z	B_{eq}
Ir	−0.14480(3)	0.23343(2)	0.22703(3)	1.72(2)
Co	0.0	0.0	0.0	1.60(5)
S1	0.0905(2)	0.1732(2)	0.1152(2)	2.04(7)
S2	−0.0587(2)	0.0391(2)	0.2564(2)	2.03(7)
S3	−0.2426(2)	0.1374(2)	−0.0321(2)	2.01(7)
N1	−0.1982(10)	0.4003(7)	0.1743(11)	2.75(31)
N2	−0.0310(10)	0.2922(7)	0.4695(9)	2.62(30)
N3	−0.3719(9)	0.2659(7)	0.2919(11)	3.09(35)
C1	0.0260(12)	0.2840(9)	0.0020(12)	3.30(38)
C2	−0.0543(13)	0.4083(8)	0.1149(12)	3.29(37)
C3	0.1078(12)	0.0699(9)	0.4112(11)	2.85(35)
C4	0.0412(14)	0.1908(11)	0.5383(11)	3.28(39)
C5	−0.4018(13)	0.1076(10)	0.0275(15)	3.60(43)
C6	−0.4817(15)	0.2264(15)	0.1518(18)	4.82(58)
O1W	0.2444(14)	0.3993(9)	0.5128(13)	5.10(47)
N1N	−0.3421(11)	0.4461(11)	0.7437(11)	3.91(41)
N2N	0.5100(33)	0.1012(51)	0.4931(33)	9.1(21)
				B
O11	−0.4301(16)	0.4686(13)	0.8481(16)	7.08(28)
O12	−0.4074(22)	0.4905(18)	0.6151(23)	10.16(45)
O13	−0.2091(28)	0.4370(22)	0.7657(29)	12.48(60)
O21	0.4705(29)	0.0553(23)	0.5967(31)	6.43(49)
O22	0.5444(40)	0.0054(33)	0.3664(43)	9.30(80)
O23	0.5303(22)	0.2005(18)	0.5499(23)	4.20(31)

hydrogen atoms are given in Table 1.[27]

Results and Discussion

Crystal Structure of $[Co\{Ir(aet)_3\}_2](NO_3)_3$ (3a$(NO_3)_3$). X-Ray structural analysis revealed the presence of a discrete trivalent complex cation, three nitrate anions, and two water molecules. Perspective drawing of the entire complex cation is given in Fig. 1 and its bond lengths and angles are listed in Table 2.

The entire complex cation consists of two approximately octahedral *fac*(*S*)-[Ir(aet)$_3$] units and one cobalt atom. The three thiolato sulfur atoms in each *fac*(*S*)-[Ir(aet)$_3$] unit coordinate to the cobalt atom, forming a linear-type S-bridged $Ir^{III}Co^{III}Ir^{III}$ trinuclear structure. The crystallographic center of symmetry located at the cobalt atom requires that the three metals are arranged to be exactly linear with the two identical Ir–Co distances (2.906(1) Å). The coordination geometry of the central cobalt atom is trigonally distorted from a regular octahedron, having the acute S–Co–S bite angles (average 84.7(1)°) (Table 2). In the terminal *fac*(*S*)-[Ir(aet)$_3$] units, the S_3 faces are compressed to give the acute S–Ir–S angles (average 84.2(1)°), while the N_3 faces are expanded to give the obtuse N–Ir–N angles (average 96.3(3)°).

The overall structure of **3a** is similar to that of the corresponding linear-type $Co^{III}Co^{III}Co^{III}$ complex, $[Co\{Co(aet)_3\}_2]^{3+}$.[5] In particular, the bond angles around the central cobalt and the terminal iridium atoms are quite similar to those around the central cobalt (average S–Co–S = 83.5(9)°) and the terminal cobalt atoms (average S–Co–S=84.5(8)° and N–Co–N= 94.6(6)°) in $[Co\{Co(aet)_3\}_2]^{3+}$, respectively. The bond distances associated with the aet ligands (average S–C= 1.816(11) Å, C–C=1.527(18) Å, and C–N=1.480(17) Å) are essentially the same as those observed in $[Co\{Co(aet)_3\}_2]^{3+}$ (average S–C = 1.821(7) Å, C–C = 1.526-

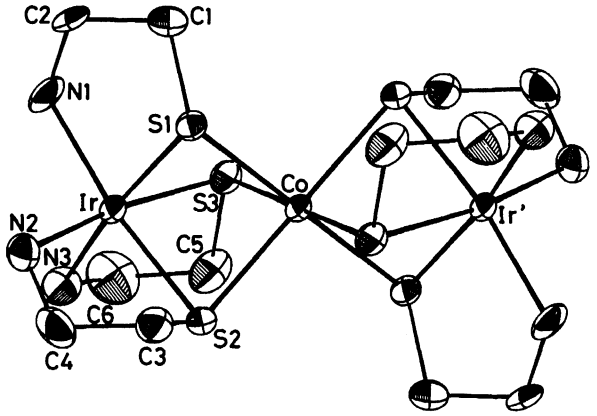

Fig. 1. Perspective view of $\Delta\Lambda$-$[Co\{Ir(aet)_3\}_2]^{3+}$ (**3a**) with the atomic labeling scheme.

Table 2. Bond Distances (Å) and Angles (°) of the Complex Cation

Ir–S1	2.310(2)	S1–C1	1.818(9)
Ir–S2	2.307(2)	S2–C3	1.833(9)
Ir–S3	2.305(2)	S3–C5	1.797(11)
Ir–N1	2.106(7)	N1–C2	1.534(13)
Ir–N2	2.147(7)	N2–C4	1.456(13)
Ir–N3	2.107(8)	N3–C6	1.449(17)
Co–S1	2.309(2)	C1–C2	1.524(13)
Co–S2	2.292(2)	C3–C4	1.525(14)
Co–S3	2.291(2)	C5–C6	1.531(18)
S1–Ir–S2	83.8(1)	Ir–S1–Co	78.0(1)
S1–Ir–S3	84.0(1)	Ir–S1–C1	95.5(3)
S2–Ir–S3	84.7(1)	Co–S1–C1	115.8(3)
S1–Ir–N1	87.9(2)	Ir–S2–Co	78.4(1)
S2–Ir–N1	171.3(2)	Ir–S2–C3	94.8(3)
S3–Ir–N1	91.8(3)	Co–S2–C3	112.0(3)
S1–Ir–N2	92.5(2)	Ir–S3–Co	78.4(1)
S2–Ir–N2	86.0(2)	Ir–S3–C5	95.8(4)
S3–Ir–N2	170.3(2)	Co–S3–C5	113.6(4)
N1–Ir–N2	97.1(3)	Ir–N1–C2	110.3(5)
S1–Ir–N3	170.0(3)	Ir–N2–C4	112.0(6)
S2–Ir–N3	92.6(2)	Ir–N3–C6	111.7(7)
S3–Ir–N3	86.3(3)	S1–C1–C2	107.9(6)
N1–Ir–N3	95.1(3)	N1–C2–C1	110.4(7)
N2–Ir–N3	96.6(3)	S2–C3–C4	106.8(7)
S1–Co–S2	84.2(1)	N2–C4–C3	112.4(7)
S1–Co–S3	84.4(1)	S3–C5–C6	106.7(8)
S2–Co–S3	85.4(1)	N3–C6–C5	112.6(10)

(12) Å, and C–N=1.489(14) Å). However, it is noted that the Co–S distances (average 2.297(2) Å) in **3a** are longer than the corresponding Co–S ones (average Co–S=2.262(11) Å) in $[Co\{Co(aet)_3\}_2]^{3+}$, which indicates that the sulfur atoms of the *fac*(*S*)-$[Ir(aet)_3]$ units bind to the central cobalt atom more weakly than do the sulfur atoms of the *fac*(*S*)-$[Co(aet)_3]$ units. The average Ir–N distance (2.120(8) Å) in **3a** is ca. 0.12 Å longer than the Co–N one (1.996(8) Å) in $[Co\{Co(aet)_3\}_2]^{3+}$, as is expected from the size difference between cobalt and iridium atoms. On the other hand, the average Ir–S bond distance (2.307(2) Å) is only ca. 0.07 Å longer than the corresponding Co–S one (average 2.238(7) Å) in $[Co\{Co(aet)_3\}_2]^{3+}$. These facts suggest that the Ir–S bonds in the *fac*(*S*)-$[Ir(aet)_3]$ units are stronger than the Co–S bonds in the *fac*(*S*)-$[Co(aet)_3]$ ones. Moreover, the average Ir–S distance in **3a** is ca. 0.03 Å shorter than that found in the related T-cage-type S-bridged octanuclear complex $[\{Ir(aet)_3\}_4Zn_{2.8}Co_{1.2}O]^{6+}$ (average 2.335(7) Å), although the Ir–N distances are in good agreement with those in $[\{Ir(aet)_3\}_4Zn_{2.8}Co_{1.2}O]^{6+}$ (average 2.12(3) Å).[17] Accordingly, it is considered that in the present S-bridged $Ir^{III}Co^{III}Ir^{III}$ complex (**3a**) each thiolato sulfur atoms strongly binds to the terminal iridium atom, which results in the weak binding to the central cobalt atom.

Considering the absolute configurations (Δ and Λ) of the two *fac*(*S*)-$[Ir(aet)_3]$ units, meso ($\Delta\Lambda$) and racemic ($\Delta\Delta$ and $\Lambda\Lambda$) isomers are possible for $[Co\{Ir(aet)_3\}_2]^{3+}$. The space group $P\bar{1}$ and $Z=1$ clearly indicate that **3a** is the meso isomer containing the Δ- and Λ-*fac*(*S*)-$[Ir(aet)_3]$ units, as shown in Fig. 1. This is consistent with the fact that **3a** was not optically resolved. All the aet chelate rings have a distinct gauche form with the λ conformation for the Δ unit and the δ conformation for the Λ unit, and therefore, all the bridging sulfur atoms are fixed to the *R* configuration for the Δ unit and the *S* configuration for the Λ unit.

Characterization. The absorption and CD spectra of **2** with the L-cys ligands are shown in Fig. 2, together with those of Δ_{LLL}-*fac*(*S*)-$[Rh(L\text{-cys-}N,S)_3]^{3-}$; the data are summarized in Table 3. **2** exhibits d–d absorption shoulders at 31.7 and 36.0×10^3 cm^{-1} and the sulfur-to-metal charge transfer (SMCT) band at 49.0×10^3 cm^{-1}. This absorption spectral behavior corresponds well with that of *fac*(*S*)-$[Rh(L\text{-cys-}N,S)_3]^{3-}$, although each absorption band of **2** commonly shifts to higher energy than that of *fac*(*S*)-$[Rh(L\text{-cys-}N,S)_3]^{3-}$. In the ^{13}C NMR spectrum, **2** gives only three signals ($\delta=34.94$, 71.13, and 179.97) due to the methylene, methine, and carboxylate carbon atoms. From these facts and elemental analysis, **2** can be assigned to either Δ_{LLL}- or Λ_{LLL}-*fac*(*S*)-$[Ir(L\text{-cys-}N,S)_3]^{3-}$ having a C_3 symmetry. The CD spectrum of **2** exhibits two negative CD bands at 28.4 and 33.1×10^3 cm^{-1} in the d–d absorption band region (Fig. 2 and Table 3). This CD spectral behavior is in good agreement with that of

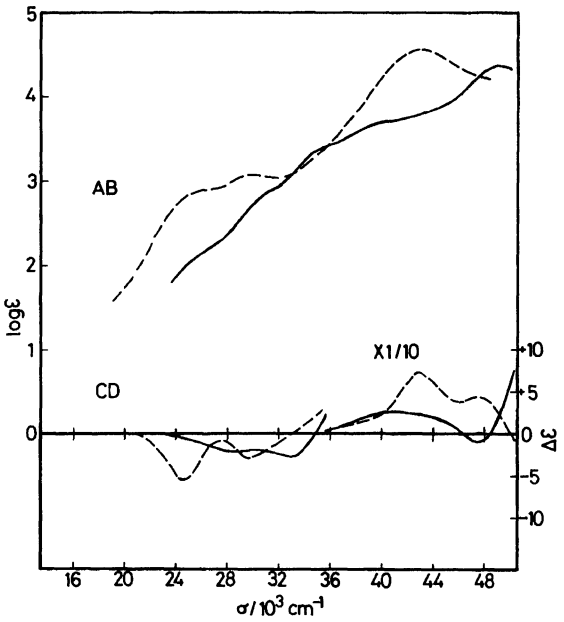

Fig. 2. Electronic absorption and CD spectra of Δ_{LLL}-*fac*(*S*)-$[Ir(L\text{-cys-}N,S)_3]^{3-}$ (**2**) (—) and Δ_{LLL}-*fac*(*S*)-$[Rh(L\text{-cys-}N,S)_3]^{3-}$ (— —).

Δ_{LLL}-*fac*(*S*)-$[Rh(L\text{-cys-}N,S)_3]^{3-}$, considering that each absorption band of **2** shifts to higher energy than that of Δ_{LLL}-*fac*(*S*)-$[Rh(L\text{-cys-}N,S)_3]^{3-}$. Accordingly, it is confidently assigned that **2** is Δ_{LLL}-*fac*(*S*)-$[Ir(L\text{-cys-}N,S)_3]^{3-}$.

1 with the aet ligands is sparingly soluble in any solvent, and therefore, its accurate extinction coefficient could not be measured. The qualitative absorption spectrum of **1** in water is quite similar to that of *fac*(*S*)-$[Ir(L\text{-cys-}N,S)_3]^{3-}$, giving absorption shoulders at 36.4 and 41.0×10^3 cm^{-1} and an absorption peak at 49.8×10^3 cm^{-1} in the higher energy region (Table 3). Taking these facts and elemental analysis into consideration, **1** is assigned to the *fac*(*S*)-$[Ir(aet)_3]$ molecule. This assignment is supported by the fact that the S-bridged trinuclear complex $[Co\{Ir(aet)_3\}_2]^{3+}$ (**3**) containing two *fac*(*S*)-$[Ir(aet)_3]$ moieties was produced using **1** as the starting mononuclear complex.

As illustrated in Fig. 3, the absorption spectrum of **3b** coincides well with that of *meso*-$[Co\{Ir(aet)_3\}_2]^{3+}$ (**3a**) over the whole region. Furthermore, **3b** was optically resolved into $(+)^{CD}_{600}$-**3b** and $(-)^{CD}_{600}$-**3b** which show CD spectra enantiomeric to each other. These facts indicate that **3b** is *rac*-$[Co\{Ir(aet)_3\}_2]^{3+}$. The CD spectral behavior of $(-)^{CD}_{600}$-**3b** resembles that of $\Delta\Delta$-$[Co\{Rh(aet)_3\}_2]^{3+}$ over the whole region (Fig. 3 and Table 3). Therefore, $(-)^{CD}_{600}$-**3b** and $(+)^{CD}_{600}$-**3b** is assignable to $\Delta\Delta$- and $\Lambda\Lambda$-$[Co\{Ir(aet)_3\}_2]^{3+}$, respectively.

The absorption spectrum of **4** with the L-cys ligands is quite similar to those of $[Co\{Ir(aet)_3\}_2]^{3+}$ over the whole region (Fig. 4 and Table 3). This indicates that **4** is the S-bridged trinuclear complex with L-cys ligands, $[Co\{Ir(L\text{-cys-}N,S)_3\}_2]^{3-}$. Three isomers,

Table 3. Absorption and CD Spectral Data of Complexes

Complex	Absorption maxima $\sigma/10^3$ cm^{-1} ($\log \varepsilon$/mol^{-1} dm^3 cm^{-1})	CD extrema $\sigma/10^3$ cm^{-1} ($\Delta\varepsilon$/mol^{-1} dm^3 cm^{-1})
Δ_{LLL}-*fac*(*S*)-[Ir(L-cys-*N*,*S*)$_3$]$^{3-}$		
	27.8 (3.3 sh)	28.41 (−2.10)
	31.7 (2.9 sh)	33.11 (−2.76)
	36.0 (3.4 sh)	40.98 (+25.14)
	41.3 (3.7 sh)	47.62 (−9.15)
	49.02 (4.37)	51.02 (+83.79)
$\Delta\Delta$-[Co{Ir(aet)$_3$}$_2$]$^{3+}$		
	16.29 (3.41)	16.18 (−33.65)
	21.1 (3.9 sh)	19.0 (+8.4 sh)
	22.88 (3.98)	21.88 (+36.95)
	33.33 (4.17)	25.97 (+7.01)
	51.81 (4.72)	32.57 (−31.32)
		36.23 (+37.46)
		39.2 (+28.2 sh)
		45.25 (+40.69)
$\Delta\Lambda$-[Co{Ir(aet)$_3$}$_2$]$^{3+}$		
	16.03 (3.32)	
	22.88 (4.07)	
	33.11 (4.14)	
	42.4 (3.9 sh)	
	50.51 (4.65)	
Δ_{LLL}-[Co{Ir(L-cys-*N*,*S*)$_3$}$_2$]$^{3-}$		
	16.26 (3.34)	16.23 (−33.16)
	21.7 (4.0 sh)	18.5 (+9.4 sh)
	22.94 (3.99)	21.93 (+38.41)
	32.89 (4.23)	26.04 (+8.92)
	50.76 (4.60)	32.47 (−21.62)
		35.71 (+41.90)
		41.32 (−11.53)
		45.05 (+35.08)

The sh label denotes a shoulder.

$\Delta_{LLL}\Delta_{LLL}$ (D_3 symmetry), $\Lambda_{LLL}\Lambda_{LLL}$ (D_3 symmetry), and $\Delta_{LLL}\Lambda_{LLL}$ (C_3 symmetry), are possible for [Co{Ir(L-cys-*N*,*S*)$_3$}$_2$]$^{3-}$. The CD spectral behavior of **4** is in good agreement with that of $\Delta\Delta$-[Co{Ir(aet)$_3$}$_2$]$^{3+}$ over the whole region, implying that **4** is $\Delta_{LLL}\Delta_{LLL}$-[Co{Ir(L-cys-*N*,*S*)$_3$}$_2$]$^{3-}$ having a D_3 symmetry. Consistent with this assignment, the ^{13}C NMR spectrum of **4** gives only three signals (δ=37.22, 69.72, and 178.72) due to the methylene, methine, and carboxylate carbon atoms for the six L-cys ligands.

The absorption spectra of [Co{Ir(aet or L-cys-*N*,*S*)$_3$}$_2$]$^{3+\text{ or }3-}$ exhibit characteristic intense absorption bands (ca. 16, 23, and 33×10^3 cm^{-1}) in the visible and near-UV regions (Figs. 3 and 4). Similar intense absorption bands have commonly been observed in the absorption spectra of [Co{Rh(aet or L-cys-*N*,*S*)$_3$}$_2$]$^{3+\text{ or }3-}$ (Fig. 3).[15] Therefore, these intense absorption bands are obviously assigned as arising from the central $Co^{III}S_6$ chromophore, taking account of the absorption spectral behavior of *fac*(*S*)-[M(aet or L-cys-*N*,*S*)$_3$]$^{0\text{ or }3-}$ (M=Ir(III) or Rh(III)) in the corresponding region (Fig. 2). It is noticed that the intense absorption bands in the visible region (ca. 16 and 23×10^3 cm^{-1}) for the present Ir^{III} $Co^{III}Ir^{III}$ complexes are located at lower energy than those for the corresponding $Rh^{III}Co^{III}Rh^{III}$ complexes. This seems to reflect that the thiolato sulfur atoms in *fac*(*S*)-[Ir(aet or L-cys-*N*,*S*)$_3$]$^{0\text{ or}3-}$ possess an electron donating ability weaker than those in *fac*(*S*)-[Rh(aet or L-cys-*N*,*S*)$_3$]$^{0\text{ or }3-}$ (vide infra).

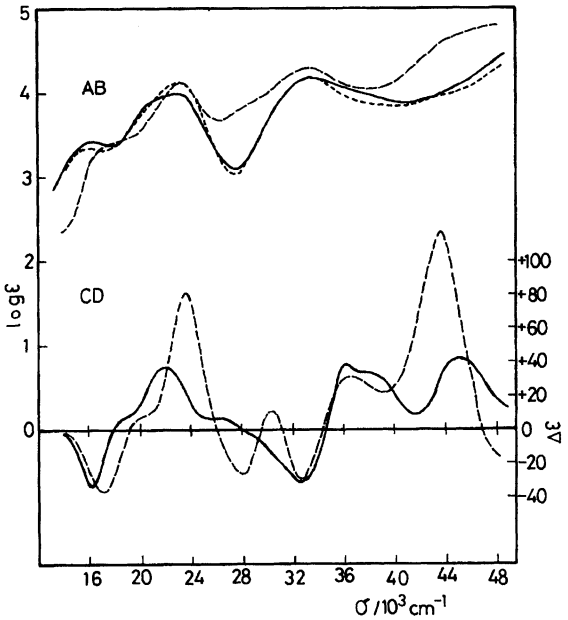

Fig. 3. Electronic absorption and CD spectra of $\Delta\Lambda$-[Co{Ir(aet)$_3$}$_2$]$^{3+}$ (**3a**) (---), $\Delta\Delta$-[Co{Ir(aet)$_3$}$_2$]$^{3+}$ ($(-)^{CD}_{600}$-**3a**) (—), and $\Delta\Delta$-[Co{Rh(aet)$_3$}$_2$]$^{3+}$ (— —).

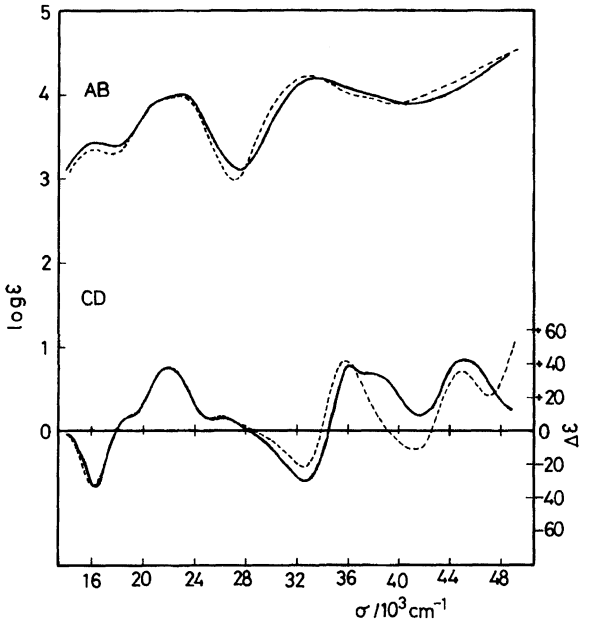

Fig. 4. Electronic absorption and CD spectra of $\Delta\Delta$-[Co{Ir(aet)$_3$}$_2$]$^{3+}$ ($(-)^{CD}_{600}$-**3a**) (—) and $\Delta_{LLL}\Delta_{LLL}$-[Co{Ir(L-cys-*N*,*S*)$_3$}$_2$]$^{3-}$ (**4**) (---).

Formation and Properties. The reactions of

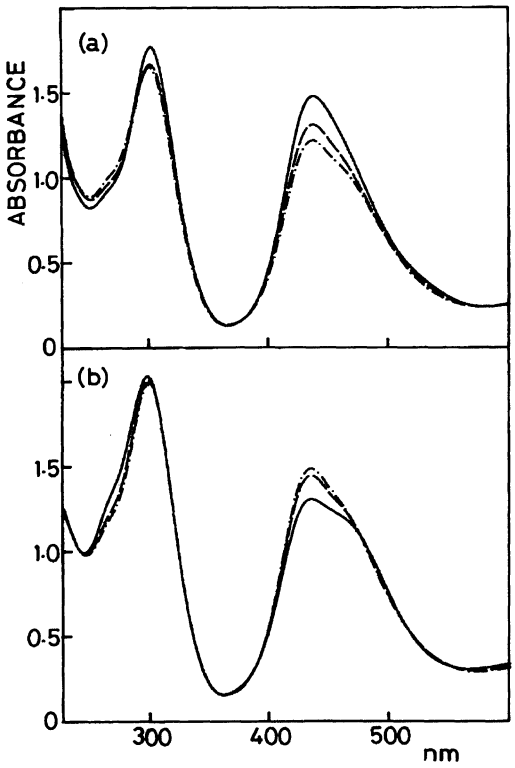

Fig. 5. Absorption spectral changes with time for *meso*-$[Co\{Ir(aet)_3\}_2]^{3+}$ in 1:1 ethanol–H_2O (a) and *rac*-$[Co\{Ir(aet)_3\}_2]^{3+}$ in D_2O (b) at room temperature; 0 h (——), 3 h (— —), and 9 h (–·–).

Fig. 6. ^{13}C NMR spectra of *rac*- (a), *meso*- (b), and $\Delta\Delta$-$[Co\{Ir(aet)_3\}_2]^{3+}$ in D_2O.

fac(*S*)-$[Ir(aet)_3]$ (**1**) or Δ_{LLL}-*fac*(*S*)-$[Ir(L\text{-cys-}N,S)_3]^{3-}$ (**2**) with Co(II), followed by the air or H_2O_2 oxidation, gave the linear-type S-bridged $Ir^{III}Co^{III}Ir^{III}$ complexes, $[Co\{Ir(aet)_3\}_2]^{3+}$ (**3**) and $\Delta_{LLL}\Delta_{LLL}$-$[Co\{Ir(L\text{-cys-}N,S)_3\}_2]^{3-}$ (**4**). The three possible isomers, $\Delta\Delta$, $\Lambda\Lambda$, and $\Delta\Lambda$, were formed for $[Co\{Ir(aet)_3\}_2]^{3+}$, which could be separated by the SP-Sephadex C-25 column chromatography. On the other hand, only the $\Delta_{LLL}\Delta_{LLL}$ isomer was formed for $[Co\{Ir(L\text{-cys-}N,S)_3\}_2]^{3-}$, even when the reaction solution of Δ_{LLL}-*fac*(*S*)-$[Ir(L\text{-cys-}N,S)_3]^{3-}$ and Co(II) was heated at 95 °C for one day, followed by the air oxidation. The configurational inversion, which gives the $\Lambda_{LLL}\Lambda_{LLL}$ and $\Delta_{LLL}\Lambda_{LLL}$ isomers besides the $\Delta_{LLL}\Delta_{LLL}$ one, has been recognized for the reaction of Δ_{LLL}-*fac*(*S*)-$[Co(L\text{-cys-}N,S)_3]^{3-}$ with Co(II) at room temperature[8,12,13] and for the reaction of Δ_{LLL}-*fac*(*S*)-$[Rh(L\text{-cys-}N,S)_3]^{3-}$ with Co(II) at 95 °C,[15] because of the dissociation followed by the rearrangement of the L-cys ligands in Δ_{LLL}-*fac*(*S*)-$[M(L\text{-cys-}N,S)_3]^{3-}$ (M=Co(III) or Rh(III)). Therefore, it is seen that Δ_{LLL}-*fac*(*S*)-$[Ir(L\text{-cys-}N,S)_3]^{3-}$ is much inert than the corresponding Co(III) and Rh(III) complexes.

The aet and L-cys $Ir^{III}Co^{III}Ir^{III}$ complexes are fairly stable in H_2O; little absorption and CD spectral changes with time were recognized at room temperature for several days. In contrast, in D_2O, methanol–H_2O, and ethanol–H_2O *meso*- and *rac*-$[Co\{Ir(aet)_3\}_2]^{3+}$ exhibited absorption spectral changes with time at room temperature. Figure 5 shows the representative absorption spectral changes of the meso isomer ((a); in 1:1 ethanol–H_2O) and the racemic isomer ((b); in D_2O). The absorption spectra of both solutions became almost constant after ca. 9 h to give the same absorption curves as each other. From the SP-Sephadex C-25 column chromatography it was found that the meso and racemic isomers coexist in each solution after 9 h, indicating that the meso–racemic isomerization occurs for $[Co\{Ir(aet)_3\}_2]^{3+}$ in these solvents. If this isomerization is caused by the racemization of the Δ- or Λ-*fac*(*S*)-$[Ir(aet)_3]$ unit, the optically active $\Delta\Delta$ and $\Lambda\Lambda$ isomers should exhibit absorption and CD spectral changes with time. However, no significant absorption and CD spectral changes were noticed for $\Delta\Delta$- or $\Lambda\Lambda$-$[Co\{Ir(aet)_3\}_2]^{3+}$ under the same conditions. Furthermore, the ^{13}C NMR spectrum of the $\Delta\Delta$ isomer in D_2O gives only two signals (δ=33.92 and 51.96) due to two kinds of methylene carbon atoms of the aet ligands, while two minor signals (δ=33.92 and 51.96 for meso and δ=33.74 and 51.64 for racemic) besides two main signals (δ=33.74 and 51.46 for meso and δ=33.92 and 51.96 for racemic) are observed in the ^{13}C NMR spectrum for each of the meso and racemic isomers, owing to the meso–racemic isomerization during the measurements (Fig. 6). Accordingly, the meso–racemic isomerization observed for $[Co\{Ir(aet)_3\}_2]^{3+}$ is not due to the racemization of the Δ- or Λ-*fac*(*S*)-$[Ir(aet)_3]$ unit but

Table 4. Electrochemical Data ($E^{\circ\prime}=(E_{pc}+E_{pa})/2$ in V vs. Ag/AgCl) for *rac*-$[Co^{III}\{M^{III}(aet)_3\}_2]^{3+}$ (M=Ir, Rh, or Co)

Complex	$M^{IV/III}Co^{III}M^{III}$	$M^{III}Co^{III/II}M^{III}$	$M^{III}Co^{II}M^{III/II}$
$[Co\{Ir(aet)_3\}_2]^{3+}$	+0.73	−0.23	
$[Co\{Rh(aet)_3\}_2]^{3+}$	+1.01	−0.36	
$[Co\{Co(aet)_3\}_2]^{3+}$		−0.66	−0.84

At 22 °C in water (0.1 mol dm^{-3} $NaNO_3$) at a glassy-carbon electrode with scan rate 100 mV s^{-1}.

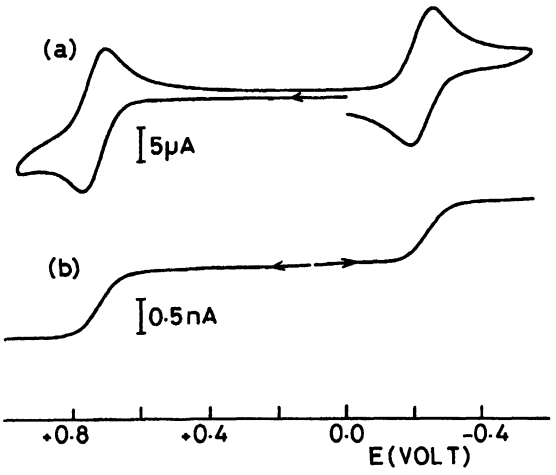

Fig. 7. Cyclic voltammogram at a glassy-carbon electrode (scan rate 100 mV s^{-1}) (a) and steady-state voltammogram at a platinum microelectrode (scan rate 10 mV s^{-1}) (b) for *rac*-$[Co\{Ir(aet)_3\}_2]^{3+}$ in water (0.1 mol dm^{-3} $NaNO_3$).

to the intermolecular exchange of the *Δ*- or *Λ*-*fac*(*S*)-$[Ir(aet)_3]$ unit, which implies the cleavage of the Co–S bonds in $[Co\{Ir(aet)_3\}_2]^{3+}$. Since the meso–racemic isomerization has not occurred for $[Co\{Co(aet)_3\}_2]^{3+}$ and $[Co\{Rh(aet)_3\}_2]^{3+}$ under the same conditions,[2,7,15] it is concluded that the Co–S bonds in $[Co\{Ir(aet)_3\}_2]^{3+}$ are weaker than those in $[Co\{Co(aet)_3\}_2]^{3+}$ and $[Co\{Rh(aet)_3\}_2]^{3+}$, presumably because of the stronger Ir–S bonds than the Co–S or Rh–S bond. This conclusion is compatible with the X-ray analytical result.

Electrochemistry. Electrochemical studies were performed for the representative *rac*-$[Co^{III}\{Ir^{III}(aet)_3\}_2]^{3+}$ together with *rac*-$[Co^{III}\{Rh^{III}(aet)_3\}_2]^{3+}$ and *rac*-$[Co^{III}\{Co^{III}(aet)_3\}_2]^{3+}$ in 0.1 mol dm^{-3} $NaNO_3$ aqueous solutions; the data are summarized in Table 4. As shown in Fig. 7(a), the cyclic voltammogram of *rac*-$[Co^{III}\{Ir^{III}(aet)_3\}_2]^{3+}$ at a grassy-carbon electrode displays two redox couples at $E^{\circ\prime}=-0.23$ V and +0.73 V in the potential region +1.1—−1.1 V (vs. Ag/AgCl). The peak current is proportional to the square root of the scan rate and the ratio of anodic to cathodic peak currents is nearly unity for each of the redox couples. At a scan rate of 100 mV s^{-1}, the observed peak separation ($E_{pc}-E_{pa}$) is 70 mV for each of the redox couples. These results establish that the two redox processes are almost reversible. In analogy to the characterized electrochemistry of the $[Co^{III}\{Co^{III}$(aet or L-cys-*N*,*S*)$_3\}_2]^{3+\text{ or }3-}$ and $[Co^{III}\{Rh^{III}$(aet or L-cys-*N*,*S*)$_3\}_2]^{3+\text{ or }3-}$ systems,[7,14,15] the redox process at $E^{\circ\prime}=-0.23$ V is assigned as the one-electron redox reaction due to the central Co(III)/Co(II). This redox potential is 130 mV more positive than that for $[Co\{Rh(aet)_3\}_2]^{3+}$ and 430 mV more positive than that for $[Co\{Co(aet)_3\}_2]^{3+}$ (Table 4), indicating that the terminal *fac*(*S*)-$[M(aet)_3]$ units make it easier to reduce the central Co(III) to Co(II) in the order M=Ir(III)>Rh(III)>Co(III). This can be ascribed to the electron-donating ability of the facially arranged thiolato atoms in the *fac*(*S*)-$[M(aet)_3]$ units, which decreases in the order M=Co(III)>Rh(III)>Ir(III).

Corresponding with the cyclic voltammogram at a grassy-carbon electrode, *rac*-$[Co\{Ir(aet)_3\}_2]^{3+}$ gives two steady-state waves ($E_{1/2}=-0.23$ V and +0.73 V vs. Ag/AgCl) at a platinum microelectrode, of which currents are roughly equal to each other (Fig. 7(b)). This indicates that the redox couple at $E^{\circ\prime}=+0.73$ V is one-electron process as is the couple at $E^{\circ\prime}=-0.23$ V. *rac*-$[Co\{Rh(aet)_3\}_2]^{3+}$ exhibits the corresponding redox couple at more positive potential ($E^{\circ\prime}=+1.01$ V), while no redox couple is observed for *rac*-$[Co\{Co(aet)_3\}_2]^{3+}$ in the positive potential region up to +1.1 V (Table 4). Considering these facts and that the Ir(III) complexes are generally oxidized more easily than the corresponding Rh(III) complexes, it is probable that the redox couple at $E^{\circ\prime}=+0.73$ V involves the terminal Ir(III)/(IV) redox process. Accordingly, the two redox couples observed for *rac*-$[Co\{Ir(aet)_3\}_2]^{3+}$ are formally represented as the metal centered reactions in Eq. 1.

$$Ir^{IV}Co^{III}Ir^{III} + e^- \rightleftharpoons Ir^{III}Co^{III}Ir^{III} + e^- \rightleftharpoons Ir^{III}Co^{II}Ir^{III} \quad (1)$$

From the separation between the two redox potentials, the comproportionation constant K_{com} defined in Eq. 2 (M=Rh or Ir) can be calculated according to a well-known treatment.[28]

$$M^{IV}Co^{III}M^{III} + M^{III}Co^{II}M^{III} \rightleftharpoons 2M^{III}Co^{III}M^{III} \quad (2)$$

The K_{com} values for $[Co\{Ir(aet)_3\}_2]^{3+}$ and $[Co\{Rh(aet)_3\}_2]^{3+}$ are 8.2×10^{16} and 2.8×10^{23}, respectively. This indicates that for the present linear-type S-bridged trinuclear complexes the equal-valence form

$M^{III}Co^{III}M^{III}$ is drastically stabilized in comparison with the mixed-valence forms $M^{IV}Co^{III}M^{III}$ and $M^{III}Co^{II}M^{III}$, although replacement of the *fac*(*S*)-[Rh(aet)$_3$] unit by the *fac*(*S*)-[Ir(aet)$_3$] one decreases the stability of the equal-valence form.

This work is supported by the Grant-in-Aid for Scientific Research No. 04640569 from the Ministry of Education, Science and Culture.

References

1) D. H. Busch and D. C. Jicha, *Inorg. Chem.*, **1**, 884 (1962).
2) G. R. Brubaker and B. E. Douglas, *Inorg. Chem.*, **6**, 1562 (1967).
3) R. E. DeSimone, T. Ontko, L. Wardman, and E. L. Blinn, *Inorg. Chem.*, **14**, 1313 (1975).
4) E. L. Blinn, P. Butlar, K. M. Chapman, and S. Harris, *Inorg. Chim. Acta*, **24**, 139 (1977).
5) M. J. Heeg, E. L. Blinn, and E. Deutsch, *Inorg. Chem.*, **24**, 1118 (1985).
6) D. W. Johnson and T. R. Brewer, *Inorg. Chim. Acta*, **151**, 221 (1988).
7) S. Miyanowaki, T. Konno, K. Okamoto, and J. Hidaka, *Bull. Chem. Soc. Jpn.*, **61**, 2987 (1988).
8) T. Konno, S. Aizawa, and J. Hidaka, *Bull. Chem. Soc. Jpn.*, **62**, 585 (1989).
9) T. Konno, K. Okamoto, and J. Hidaka, *Bull. Chem. Soc. Jpn.*, **63**, 3027 (1990).
10) T. Konno, T. Nagashio, K. Okamoto, and J. Hidaka, *Inorg. Chem.*, **31**, 1160 (1992).
11) T. Konno, K. Okamoto, and J. Hidaka, *Acta Crystallogr., Sect. C*, **49**, 222 (1993).
12) T. Konno, S. Aizawa, K. Okamoto, and J. Hidaka, *Chem. Lett.*, **1985**. 1017.
13) K. Okamoto, S. Aizawa, T. Konno, H. Einaga, and J. Hidaka, *Bull. Chem. Soc. Jpn.*, **59**, 3859 (1986).
14) S. Aizawa, K. Okamoto, H. Einaga, and J. Hidaka, *Bull. Chem. Soc. Jpn.*, **61**, 1601 (1988).
15) T. Konno, S. Aizawa, K. Okamoto, and J. Hidaka, *Bull. Chem. Soc. Jpn.*, **63**, 792 (1990).
16) T. Konno, K. Okamoto, and J. Hidaka, *Chem. Lett.*, **1990**, 1043.
17) T. Konno, K. Okamoto, and J. Hidaka, *Inorg. Chem.*, **30**, 2253 (1991).
18) K. Okamoto, T. Konno, Y. Kagayama, and J. Hidaka, *Chem. Lett.*, **1992**, 1105.
19) T. Konno, K. Okamoto, and J. Hidaka, *Inorg. Chem.*, **31**, 3875 (1992).
20) The elemental analysis suggests that the purple complex is $[Co^{II}\{Ir(aet)_3\}_2](NO_3)_2$. Found: C, 13.78; H, 3.72; N, 10.67%. Calcd for $[Co\{Ir(aet)_3\}_2](NO_3)_2\cdot 1.5H_2O$: C, 13.71; H, 3.74; N, 10.66%.
21) The purple suspension also became a dark green solution without H_2O_2, on stirring at room temperature for several hours in the air. The addition of 4 cm^3 of a saturated $NaNO_3$ solution to the dark green reaction solution, followed by storing in a refrigerator overnight, gave fine green-black crystals of **3**$(NO_3)_3$. Yield: 0.33 g (42%). Found: C, 12.95; H, 3.43; N, 11.36%. Calcd for $[Co\{Ir(aet)_3\}_2](NO_3)_3\cdot 1.5H_2O$: C, 12.95; H, 3.53; N, 11.33%.
22) The addition of a large amount ethanol to the purple solution gave the purple complex, which is assigned to $\Delta_{LLL}\Delta_{LLL}$-$[Co^{II}\{Ir(L\text{-}cys\text{-}N,S)_3\}_2]^{4-}$ from the elemental analysis and absorption and CD spectral measurement. Found: C, 15.71; H, 3.32; N, 5.79%. Calcd for $Na_4[Co\{Ir(L\text{-}cys)_3\}_2]\cdot 8H_2O$: C, 15.51; H, 3.33; N, 6.03%.
23) B. A. Frens, "The Enraf–Nonius Structure Determination Package (SDP)," Delft, Holland (1978).
24) G. M. Sheldrick, "SHELX76, Program for Crystal Structure Determination," University of Cambridge, England (1976).
25) "International Tables for X-Ray Crystallography," Kynoch Press, Birmingham (1974), Vol. IV; D. T. Cromer and J. B. Mann, *Acta Crystallogr., Sect. A*, **24**, 321 (1966).
26) $S=\{\Sigma_w(|F_o|-|F_c|)^2\}^{1/2}/(N_o-N_p)$; N_o and N_p denote number of reflections and number of refined parameters, respectively.
27) Lists of structure factors, bond distances and angles, anisotropic thermal parameters, and hydrogen atom coordinates are deposited as Document No. 66038 at the Office of the Editor of Bull. Chem. Soc. Jpn.
28) R. R. Gange, C. L. Spiro, T. J. Smith, C. A. Hamann, W. R. Thies, and A. K. Shiemke, *J. Am. Chem. Soc.*, **103**, 4073 (1981).